Nanoscale Res Lett (2010) 5:625–630
DOI 10.1007/s11671-010-9525-1

NANO EXPRESS

Microwave Synthesis of Nearly Monodisperse Core/Multishell Quantum Dots with Cell Imaging Applications

Huaipeng Su · Hengyi Xu · Shuai Gao · John David Dixon · Zoraida P. Aguilar · Andrew Y. Wang · Jian Xu · Jingkang Wang

Received: 20 June 2009 / Accepted: 5 January 2010 / Published online: 26 January 2010

Abstract We report in this article the microwave synthesis of relatively monodisperse, highly crystalline CdSe quantum dots (QDs) overcoated with $Cd_{0.5}Zn_{0.5}S$/ZnS multishells. The as-prepared QDs exhibited narrow photoluminescence bandwidth as the consequence of homogeneous size distribution and uniform crystallinity, which was confirmed by transmission electron microscopy. A high photoluminescence quantum yield up to 80% was measured for the core/multishell nanocrystals. Finally, the resulting CdSe/$Cd_{0.5}Zn_{0.5}S$/ZnS core/multishell QDs have been successfully applied to the labeling and imaging of breast cancer cells (SK-BR3).

Keywords Microwave · Semiconductor · Quantum Dots · Photoluminescence · Cell labeling

Introduction

The potential biological applications of colloidal semiconductor nanocrystals have been gaining more and more interest, since they were first reported by Alivisatos and Nie groups [1, 2]. Compared with traditional organic dyes, semiconductor quantum dots (QDs) have exceptional intrinsic properties including high photoluminescence quantum yield, narrow fluorescence emission, long fluorescence lifetime, large effective Stokes shifts, and tunable excitation wavelength, making them very appealing for various biological applications [3–5]. Therefore, the development of simple, low-cost, and scalable synthetic methods for the mass production of monodisperse, stable, and size/shape-controlled nanocrystals will be very important.

Efforts have been devoted to the preparation, surface functionalization, and various biological applications of colloidal nanocrystals over the past two decades. Various synthetic approaches have been explored to produce colloidal nanocrystals with uniform size and shape [6–8]. The so-called hot injection method, which involves injecting a reactant precursor solution into a reactor containing a mixture of other reactants and surfactants at high temperature, has been one of the most successful and popular approaches, since the synthesis of high-quality semiconductor QDs was first reported [6]. The fast introduction of precursor solution initiates a short burst of homogeneous nucleation that is stopped with a sudden decrease in temperature to prevent excess nucleation which is favorable for the succeeding growth of the initially formed nuclei. Thus, monodisperse, highly crystalline nanocrystals are usually prepared using this method, and in some cases, with some evolutional improvements [9, 10].

The "hot injection" method, however, utilizes conventional convective heating that can lead to nonuniform reaction conditions caused by sharp thermal gradients in the bulk solution. Bulk scale reactions are more affected by this heating process because of the large volume and heat stability during injections. Enormous effort has been made to overcome these problems [8, 11–13]. One method found to be effective and convenient is by using microwave

H. Su · S. Gao · J. Wang (✉)
State Key Laboratory of Chemical Engineering, School of Chemical Engineering and Technology, Tianjin University, Tianjin 300072, People's Republic of China
e-mail: wangjkch@tju.edu.cn

H. Su · H. Xu · J. D. Dixon · Z. P. Aguilar · A. Y. Wang
Ocean NanoTech LLC, 2143 Worth Lane, Springdale, AR 72764, USA

H. Su · J. Xu
Department of Engineering Science and Mechanics, Penn State University, University Park, PA 16802, USA

heating during synthesis. Irradiation with a microwave instead of convective heating overcomes heterogeneity of the heat distribution in the solution. Gerbec and co-workers studied microwave heating method and successfully prepared InGaP, InP, and CdSe nanoparticles [13]. Roy et al. reported microwave synthesis of the core CdSe QDs and coated them with ZnS [14]. However, the nanocrystals prepared with their methods were characterized with large full-width-at-half-maximum (FWHM) bandwidths (36–70 nm). Moreover, in many cases [15, 16], the crystallinity and optical properties of the nanoparticles appeared to be of low grade.

By overcoating with layers of shell to establish a core/shell/shell system, such as CdSe/CdS/ZnS [17, 18] and CdSe/ZnSe/ZnS [19, 20], nanocrystals have been shown to be generally more robust and of higher photoluminescence quantum yield (PLQY). In this paper, we present the synthesis of relatively monodisperse, highly crystalline CdSe QDs using microwave heating followed by the conventional shell-growth method to produce CdSe/$Cd_{0.5}Zn_{0.5}S$/ZnS core/multishell QDs. The microwave-synthesized CdSe nanocrystal cores exhibited high crystallinity and narrow size distribution (FWHM, $\sim$25 nm). Moreover, the resulting CdSe/$Cd_{0.5}Zn_{0.5}S$/ZnS core/multishell QDs were measured with a high PLQY up to 80%. The core/multishell QDs were successfully applied to the labeling and imaging of cancer cells, exhibiting great promise for biological applications.

Experimental

Materials

Cadmium oxide (99.99%), zinc oxide (99.9%), selenium (99.999%, 200 mesh), sulfur (99.999%, powder), tributylphosphine (TBP, 93%), and n-octadecylphosphonic acid (ODPA, 98%) were purchased from Alfa Aesar. Trioctylphosphine oxide (TOPO, 90%), 1-octadecene (ODE), oleic acid (OA, 90%), octadecylamine (ODA, 97%), n-(3-dimethylaminopropyl)-n'-ethylcarbodiimide hydrochloride (EDC), n-hydroxysulfosuccinimide sodium salt (sulfo-NHS) and Dulbecco's phosphate-buffered saline (DPBS) were obtained from Sigma–Aldrich. All organic solvents were purchased from EM Sciences. All chemicals were used directly without any further purification.

Preparation of CdSe Core

For the synthesis of CdSe cores, ODA, and TOPO were used as the ligands. Cadmium precursor was prepared by conventional heating of a mixture of 0.24 mmol of CdO, 0.51 mmol of ODPA, and 9.8 g of ODE to 300°C for 15 min to form an optically clear solution. Selenium precursor was prepared by dissolving 0.173 g of Se powder in 0.893 g of TBP in nitrogen environment. Both precursors were used in the microwave nanoparticle synthesis that was carried out in a H2800 microwave processor (Energy Beam Sciences, Inc., USA) equipped with a thermometer.

For the microwave synthesis of CdSe QDs, 1.1 ml of the Se precursor solution was injected into a 100-ml sealed flask containing 10 g of Cd precursor, 9 g of ODA, and 1.5 g of TOPO, which had been degassed in nitrogen. This mixture was microwaved to 50°C for 15 min to melt all the solids into a homogeneous solution. The solution was microwave heated up to 200°C at the maximum power (800 W) after which the microwave power was set at 400 W in order to keep the reaction temperature constant for a period of time to reach the desired size. Once the corresponding QD size was attained, the microwave was turned off, and the mixture was allowed to cool down to room temperature before being taken out of the microwave oven. Hexane was added to disperse the CdSe QDs, which were then purified by repeated acetone precipitation.

Preparation of CdSe/$Cd_{0.5}Zn_{0.5}$/ZnS Core/Multishell QDs

CdSe/$Cd_{0.5}Zn_{0.5}$/ZnS core/multishell QDs were synthesized under conventional convective heating in order to apply the successive ion layer adsorption and reaction (SILAR) method [21] with slight modification. Less toxic reactant precursors, including metal oxide and elemental sulfur, were used to grow shells. The precursor solutions were prepared as reported previously [22] with the necessary doses for each monolayer growth calculated from the particle size and concentration according to the method developed by Peng et al. [23].

A typical synthesis was performed as follows: 1.3×10^{-6} mol of purified CdSe core QDs dissolved in 30 g of ODE, and 10.0 g of ODA was loaded into a 100-ml flask and heated on a heating mantle to 120°C for 15 min under nitrogen. The mixture was heated to 210°C to grow the shells at 15 min for each injection. The amounts of shell precursor injection solutions for the first two layers of $Cd_{0.5}Zn_{0.5}S$ and the third layer of ZnS were 0.74, 1.6, and 2.9 ml, respectively. Finally, the solution was cooled to 150°C for 40 min and then allowed to reach room temperature. The core/multishell QDs were purified several times by extracting with hexane and precipitating with acetone.

Bioconjutation of Core/Multishell QDs

Surface modification of the purified QDs was performed using a previously reported method [24]. This method

converts the QDs into water-soluble and biocompatible nanocrystals.

The water-soluble QDs were conjugated with goat-anti-mouse antibody (Rockland, USA) using N-(3-dimethyl-aminopropyl)-N′-ethylcarbodiimide hydrochloride (EDC) as the coupling agent. Briefly, 1 mg of N-hydroxysulfosuccinimide sodium salt (sulfo-NHS) and 2 mg of EDC were mixed with 1 ml QDs water solution (100 nM). To this was added a 0.5 mg of goat-anti-mouse antibody dissolved in deionized water with vigorous stirring for 2.0 h at room temperature. The antibody-conjugated QDs were purified by dialyzing in 50 mM borate buffer.

Cell Imaging of Core/Multishell QDs

The secondary antibody (goat anti-mouse antibody)-conjugated CdSe/$Cd_{0.5}Zn_{0.5}$/ZnS QDs was used to create fluorescent images of breast cancer cells, SK-BR3. To carry this process out, 0.1 ml of SK-BR3 suspension at a cell concentration of 1×10^6 cells/ml in DPBS was transferred into a sterile Eppendorf tube. A 1-μg sample of anti-EpCAM (Epithelial cell adhesion molecule) was added to the SK-BR3 cells and incubated for 30 min at 37°C. The cells were washed 3 times with 1 ml DPBS and precipitated at 3000 rpm for 5 min. The pelleted cells were resuspended in 50 μl DPBS. The anti-EpCAM-labeled cells were exposed to 50 pmol of QDs-goat-anti-mouse antibody conjugates and incubated for another 30 min at 37°C. The cells were washed three times with 1 ml Ocean blocking buffer B (Ocean Nanotech LLC, USA) to remove the non-attached QDs-goat-anti-mouse antibody conjugates. The washed cells were finally resuspended in 20 μl DPBS and imaged.

Characterization

UV–vis absorption spectra were collected with an HP 8453 UV/vis spectrometer. Photoluminescence (PL) and photoluminescence excitation (PLE) spectra were measured on a Perkin Elmer Lambda LS 50B luminescence spectrometer. PL spectra were recorded at an excitation wavelength of 400 nm, and excitation spectra were measured at the wavelength of the fluorescence maximum [25]. PL quantum yields were determined using a conventional method by comparison of the integrated fluorescence intensity with that of standard dye solutions. X-ray diffraction (XRD) patterns were obtained using a Rigaku D/max-gB diffractometer. Transmission electron microscopy (TEM) and high-resolution (HR) TEM images were recorded on a JEOL 100CX electron microscope operated at 80 kV and a Philips CM 200 electron microscope operated at 200 kV, respectively. For cell imaging, the QD-labeled cells were dropped onto a hemocytometer and observed under an Emscope fluorescence microscope.

Results and Discussion

Gerbec et al. [13] found that the microwave heating rates varied for different solvent and reactants. The study of effect of solvent and reactants is out of this work. Here, the heating rates in different microwave synthesis of CdSe nanocrystals were similar due to the same solvent and reactants. The microwave heating rate of a typical microwave synthesis when going from 50 to 200°C is shown in Fig. 1.

The size of CdSe QDs synthesized using microwave heating could be tuned by changing radiation time at 200°C. Figure 2 illustrates the PL peak positions of CdSe QDs synthesized at various times. Radiation times were based upon the time at 200°C. Systematic shifts of the PL peak positions toward lower energy as the radiation time increased were observed, which meant the CdSe QDs grew up. Because CdSe QDs were reproducibly prepared in this microwave synthesis method, we use the relationship between PL peak positions and radiation time shown in Fig. 2 to estimate the size of CdSe QDs in the following microwave synthesis. Once the corresponding QD size was attained, the microwave was turned off to terminate the growth of CdSe nanocrystals.

The absorption, PL and PLE spectra of microwave-synthesized CdSe nanocrystal cores, and the evolutional change of the optical properties during the growth of $Cd_{0.5}Zn_{0.5}S$/ZnS core/multishells are shown in Fig. 3. For the microwave-synthesized CdSe cores, sharp absorption excitonic features can be recognized up to the third orders, revealing the high optical quality of the CdSe cores. The

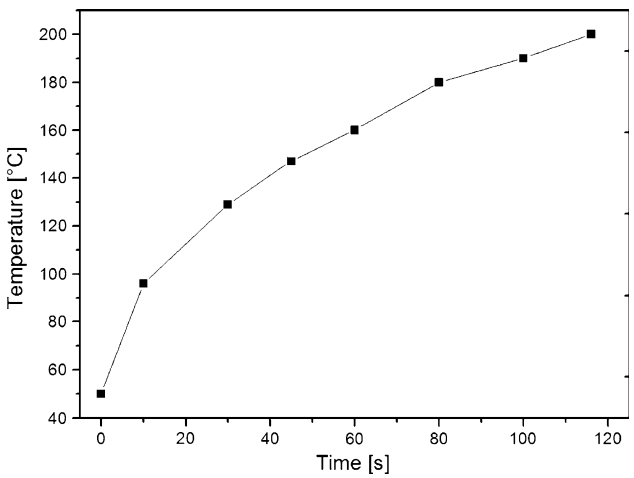

Fig. 1 Microwave heating rate of a typical microwave synthesis when going from 50 to 200°C

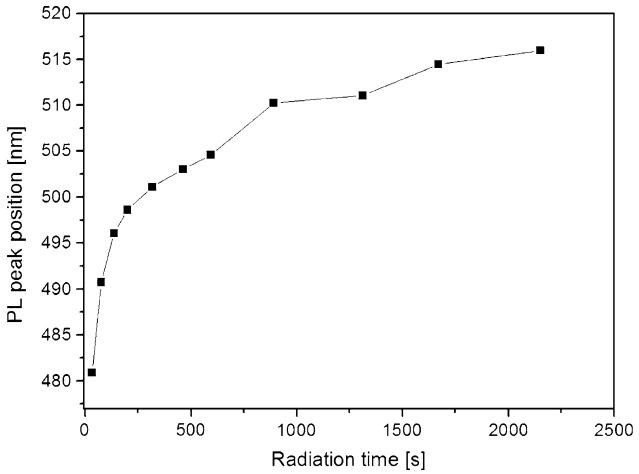

Fig. 2 PL peak positions of CdSe QDs synthesized at various radiation times

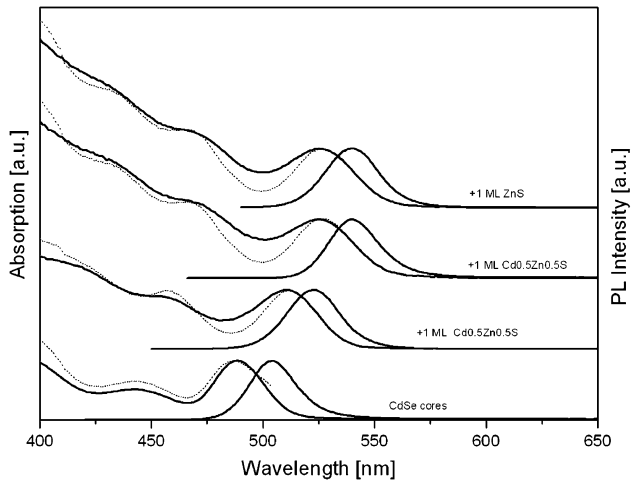

Fig. 3 Representative UV/vis absorption, PL and PLE (*dotted line*) spectra of CdSe nanocrystal cores, and CdSe/$Cd_{0.5}Zn_{0.5}S$/ZnS core/multishell QDs

corresponding PL FWHM bandwidth was only ~25 nm which is the narrowest among all reported values for microwave-synthesized QDs [14]. After the shell overcoating, there is a redshift of the excitonic absorption peaks due to the reduced energy quantization as well as the spreading of the respective wave function into the shell [26]. Systematic shift of the PL peak positions toward lower energy was, however, only observed following the growth of inner shells. There was no obvious shift after adding the outer layer of ZnS. This may be explained by the partial formation of $Zn_xCd_{1-x}S$ alloy shells [22]. Although the PL FWHM bandwidth increased after shell overcoating, it was still under 35 nm.

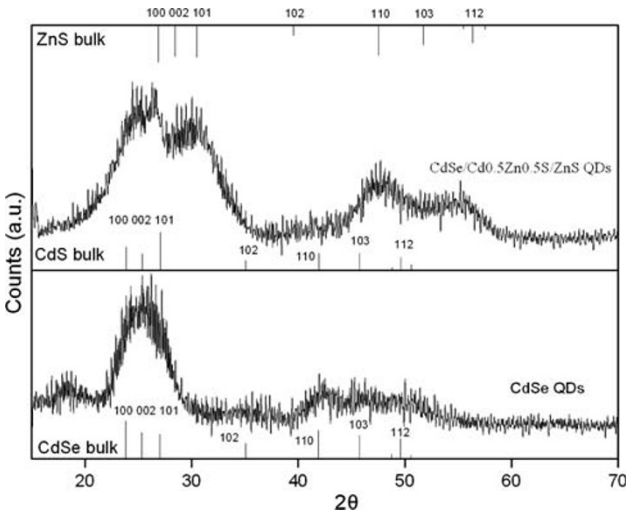

Fig. 5 Powder XRD patterns of microwave-synthesized CdSe QDs (*bottom*) and CdSe/$Cd_{0.5}Zn_{0.5}S$/ZnS core/multishell QDs (*top*)

Accompanied by the long wavelength shift of PL was a large increase in PLQY. The PLQY of the CdSe QDs was found to be 30%, which increased to above 80% for CdSe/$Cd_{0.5}Zn_{0.5}S$/ZnS core/multishell QDs. The PL emission of the core/multishell QDs was clearly visible to the naked eye under white light and a UV lamp. This again shows that the microwave-synthesized CdSe cores were of good quality which is essential for the preparation of highly fluorescent core/shell QD materials. In addition, large Stokes shifts can be observed for both the CdSe cores and CdSe/$Cd_{0.5}Zn_{0.5}S$/ZnS core/multishell QDs (Fig. 3). The PLE spectra of the

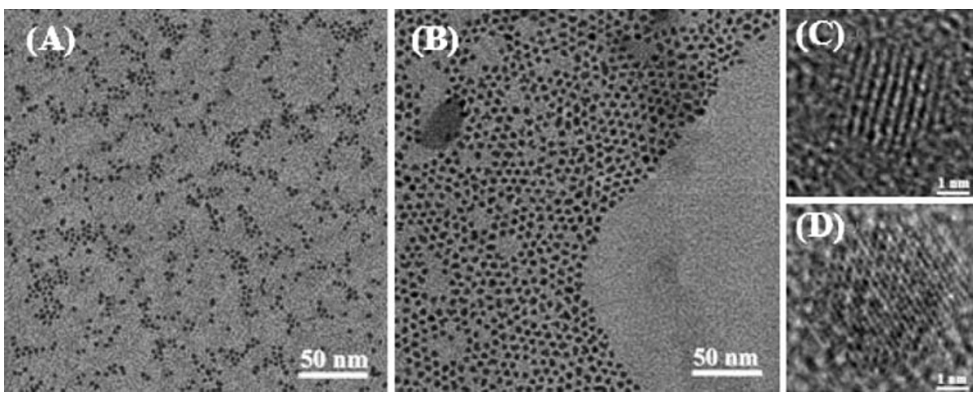

Fig. 4 Transmission electron microscopy (TEM) (**a**, **b**) and high-resolution TEM (HRTEM) (**c**, **d**) images of CdSe QDs (**a**, **c**) and CdSe/$Cd_{0.5}Zn_{0.5}S$/ZnS core/multishell QDs (**b**, **d**)

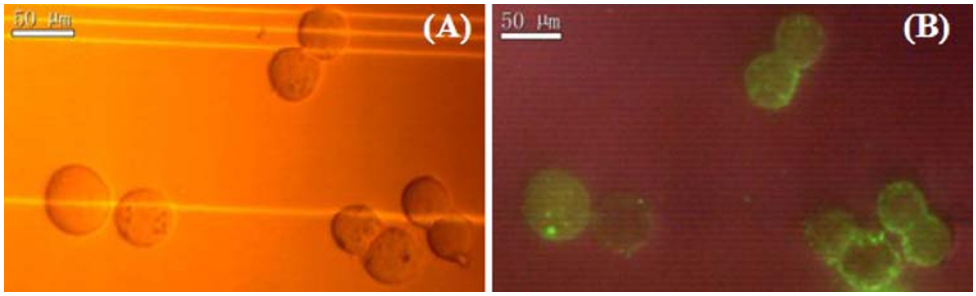

Fig. 6 Photomicrophic images of breast cancer cells (SK-BR3). The round-shaped cells were reflectively imaged under white light illumination (**a**), and after QD-labeling, the cells were with bright green florescence and easy to distinguish under UV light (**b**). (200× magnification)

microwave-synthesized QDs were also shown in Fig. 3 (dotted line). The spectra were normalized to the intensity of the first exciton absorption peak, which allowed a direct comparison between PLE and absorption. For CdSe nanocrystal cores, the PLE spectrum and absorption spectrum were highly consistent and exhibited similar excitonic features, which further verified the high-quality of microwave-synthesized CdSe crystal cores. After the growth of shells, the PLE spectrum deviated slightly from the corresponding absorption spectrum, especially at the short wavelength side of the first-order excitonic feature; this can be explained by the different shell contributions to PLE and absorption [27]. However, the PLE spectra still largely resembles the features of the corresponding absorption spectra, again, confirming the good quality of the microwave-synthesized CdSe cores and core/shell QDs.

The transmission electron microscopy (TEM) and high-resolution TEM (HRTEM) images of the CdSe QDs and CdSe/$Cd_{0.5}Zn_{0.5}S$/ZnS core/multishell QDs are presented in Fig. 4. These images showed that both the core and core/multishell QDs exhibit spherical shapes with homogeneous size distributions, suggestion that the initial size distribution of the cores was preserved during the shell growth. The measured mean sizes were 2.7 ± 0.2 nm for CdSe cores and 4.3 ± 0.3 nm for CdSe/$Cd_{0.5}Zn_{0.5}S$/ZnS core/multishell QDs, respectively. Besides, the lattice fringes were clearly displayed in the HRTEM images, which further verified the high crystallinity of these nanocrystals.

The XRD patterns of CdSe QDs and CdSe/$Cd_{0.5}Zn_{0.5}S$/ZnS core/multishell QDs are shown in Fig. 5. For CdSe cores, the peak positions agree well with the standard values of the wurtzite bulk CdSe. After overcoating with both $Cd_{0.5}Zn_{0.5}S$ and ZnS shells, the diffraction patterns shifted to higher angles, suggesting that the lattice of the nanocrystals became closer to the corresponding wurtzite structure of bulk materials of shells due to the large volume fraction of the shells in the total volume. The size of the crystal domain was calculated using the Scherrer equation, giving about the values of ~2.6 nm from (002) peak for CdSe cores and 4.0 nm for core/multishell QDs from (110) peak, which was consistent with the TEM results discussed above.

In order to show their biological applications, the core/mutilshell QDs were used to label breast cancer cells. As shown in Fig. 6, the cell imaging was bright and specific. The ring-shaped green fluorescence indicates that most of the QDs have been attached to the surface of the cell membrane. The QD-labeled fluorescent cells were stable under 4°C even after 48 h storage in DPBS, with most of the cells keeping their shapes and bright green fluorescence.

Conclusion

In summary, we have prepared relatively monodisperse CdSe QDs through the microwave heating method. The prepared CdSe nanocrystal cores exhibited narrow band photoluminescence with homogeneous size distributions and uniform crystallinity under TEM and HRTEM. The HRTEM images supported the superior quality of the microwave-synthesized CdSe/$Cd_{0.5}Zn_{0.5}S$/ZnS core/multishell QDs, which was further confirmed with the high PLQY up to 80%. Finally, the QDs were successfully employed to label and image breast cancer cells (SK-BR3) showing promise for use in biological studies.

References

1. M. Bruchez, M. Moronne, P. Gin, S. Weiss, A.P. Alivisatos, Science **281**, 2013 (1998)
2. W.C.W. Chan, S. Nie, Science **281**, 2016 (1998)
3. B.O. Dabbousi, J. Rodriguez-Viejo, F.V. Mikulec, J.R. Heine, H. Mattoussi, R. Ober, K.F. Jensen, M.G. Bawendi, J. Phys. Chem. B **101**, 9463 (1997)
4. C.A. Leatherdale, W.-K. Woo, F.V. Mikulec, M.G. Bawendi, J. Phys. Chem. B **106**, 7619 (2002)
5. W. Cai, D.-W. Shin, K. Chen, O. Gheysens, Q. Cao, S.X. Wang, S.S. Gambhir, X. Chen, Nano Lett. **6**, 669 (2006)
6. C.B. Murray, D.J. Norris, M.G. Bawendi, J. Am. Chem. Soc. **115**, 8706 (1993)
7. M.G. Bawendi, M.L. Steigerwald, L.E. Brus, Annu. Rev. Phys. Chem. **41**, 477 (1990)

8. M.A. Malik, N. Revaprasadu, P. O'Brien, Chem. Mater. **13**, 913 (2001)
9. T. Hyeon, Chem. Commun. 927 (2003)
10. L. Qu, Z.A. Peng, X. Peng, Nano Lett. **1**, 333 (2001)
11. Y.C. Cao, J. Wang, J. Am. Chem. Soc. **126**, 14336 (2004)
12. N. Pradhan, S. Efrima, J. Am. Chem. Soc. **125**, 2050 (2003)
13. J.A. Gerbec, D. Magana, A. Washington, G.F. Strouse, J. Am. Chem. Soc. **127**, 15791 (2008)
14. M.D. Roy, A.A. Herzing, S.H.D.P. Lacerda, M.L. Becker, Chem. Commun. 2106 (2008)
15. S. Verma, P.A. Joy, Y.B. Khollam, H.S. Potdar, S.B. Deshpande, Mater. Lett. **58**, 1092 (2004)
16. F. Bensebaa, F. Zavaliche, P. L'Ecuyer, T.V.R.W. Cochranec, J. Colloid Interface Sci. **277**, 104 (2004)
17. L. Manna, E.C. Scher, L.S. Li, A.P. Alivisatos, J. Am. Chem. Soc. **124**, 7136 (2002)
18. S. Jun, E. Jang, J.E. Lim, Nanotechnology **17**, 3892 (2006)
19. D.V. Talapin, I. Mekis, S. Gotzinger, A. Kornowski, O. Benson, H. Weller, J. Phys. Chem. B **108**, 18826 (2004)
20. P. Reiss, S. Carayon, J. Bleuse, A. Pron, Synth. Met. **139**, 649 (2003)
21. J.J. Li, Y.A. Wang, W. Guo, J.C. Keay, T.D. Mishima, M.B. Johnson, X. Peng, J. Am. Chem. Soc. **125**, 12567 (2003)
22. R. Xie, U. Kolb, J. Li, T. Basche, A. Mews, J. Am. Chem. Soc. **127**, 7480 (2005)
23. W.W. Yu, L. Qu, W. Guo, X. Peng, Chem. Mater. **15**, 2854 (2003)
24. L. Yang, H. Mao, Y.A. Wang, Z. Cao, X. Peng, X. Wang, H. Duan, C. Ni, Q. Yuan, G. Adams, M.Q. Smith, W.C. Wood, X. Gao, S. Nie, Small **5**, 235 (2009)
25. W. Hoheisel, V.L. Colvin, C.S. Johnson, A.P. Alivisatos, J. Chem. Phys. **101**, 8455 (1994)
26. D. Dorfs, T. Franzl, R. Osovsky, M. Brumer, E. Lifshitz, T.A. Klar, A. Eychmuller, Small **4**, 1148 (2008)
27. M. Danek, K.F. Jensen, C.B. Murray, M.G. Bawendi, Chem. Mater. **8**, 173 (1996)